



The effects of heat treatment on the mechanical properties of cold-sprayed coatings



Renzhong Huang, Michiyoshi Sone, Wenhua Ma, Hirotaka Fukanuma

Plasma Giken Co. Ltd., Toshima, Tokyo, Japan

ARTICLE INFO

Article history:

Received 7 March 2014

Accepted in revised form 5 November 2014

Available online 14 November 2014

Keywords:

Cold spray

Tensile strength

Elongation

Fracture surface

Heat treatment

ABSTRACT

In the cold spray process, deposition of particles takes place through intensive plastic deformation upon impact in a solid state at temperatures well below their melting point. Therefore, spray particles experience little oxidation or decomposition during this process. As a result, cold-sprayed coatings have excellent mechanical, electrical and thermal properties. In this work, pure Al, Cu, Ti and stainless steel 316 were deposited by cold spray. The tensile strength and elongation of these coatings were also measured. The results showed that the as-sprayed coatings of the four materials have poor ductility and almost no elongation. However, heat treatment can improve the mechanical properties of the cold-sprayed coatings to some extent. Here, the effects of heat treatment conditions on the mechanical properties of the four cold-sprayed materials are discussed.

© 2014 Elsevier B.V. All rights reserved.

1. Introduction

Cold spray is an emerging spray coating technology that was first developed in the mid 1980's at the Institute of Theoretical and Applied Mechanics in the former Soviet Union [1]. Compared to the traditional thermal spray processes, the most distinct characteristic of cold spray processing is its lower processing temperature; consequently lower thermal effects to the processed materials. Therefore, cold spray is particularly suitable to prepare coatings that are sensitive to oxidation or applications in the fields in which oxidation and thermal influences during the coating process have to be avoided [2]. So far, cold spray has been used to spray not only ductile materials such as copper [3,4], aluminum [5], nickel [6], nickel-based alloys [7], zinc; [8] but also metal matrix composites [9,10], cermets [11,12] and ceramic materials [13].

The most prominent property of cold-sprayed coatings is its low oxidation. Moreover, cold-sprayed coatings can be extremely dense under suitable spray conditions where the particles experience intensive plastic deformation. Dense coatings with low-oxidation will also mean that they have excellent mechanical, thermal and electrical properties [14,15]. Therefore, the coating deposited by cold spray is a strong candidate to apply as a structural component in the industrial field. However, the temperature history of particles during deposition processing generates some residual tensile stress due to thermal effects [15,16]. Moreover, the severe impact deformation generates some residual compressive stress due to the kinetic effects [16–19]. The intensive plastic deformation of particles also decreases the ductility of cold-

sprayed coatings due to work hardening effects. The existence of residual stress and work hardening in cold-sprayed coating decreases its mechanical, thermal and electrical properties. Some researches about the improvement of cold-sprayed coating via heat treatment were reported [14,15,20–24]. Heat treatment can effectively change the microstructure of cold-sprayed Cu [14,15,20], Al [21], stainless steel coatings [22,23] and Inconel 718 [24]. The thermal and electric conductivity of cold-sprayed coatings increased owing to the improved contact of particle-to-particle interface and the micro-hardness decreased owing to the removal of work hardening after heat treatment [14,20]. Moreover, the mechanical properties (tensile strength, elongation and tec.) of cold-sprayed coatings improved via heat treatment [15,23,24] and even demonstrated similar performance as bulk materials [15]. The previous studies paid major attention on the improvement of the mechanical properties via heat treatment. However, the determinants of the coatings' mechanical properties are still undefined up to now.

In the present study, four typical materials of Al, Cu, Ti and stainless steel were deposited by cold spray and their mechanical properties were tested. Moreover, the effects of heat treatment temperature on coating microstructures and mechanical properties were also investigated. The relationship between the porosity of cold-sprayed coatings and their mechanical properties was discussed.

2. Experimental procedures

2.1. Feedstock powder and cold spray process

Commercially available Al (>99.7%), Cu (>99.7%), Ti (Grade 2) and stainless steel 316 powders are used in the study and their morphologies are presented in Fig. 1(a)–(d). The pure Al and Ti powders show

E-mail address: rz_huang@plasma.co.jp (R. Huang).

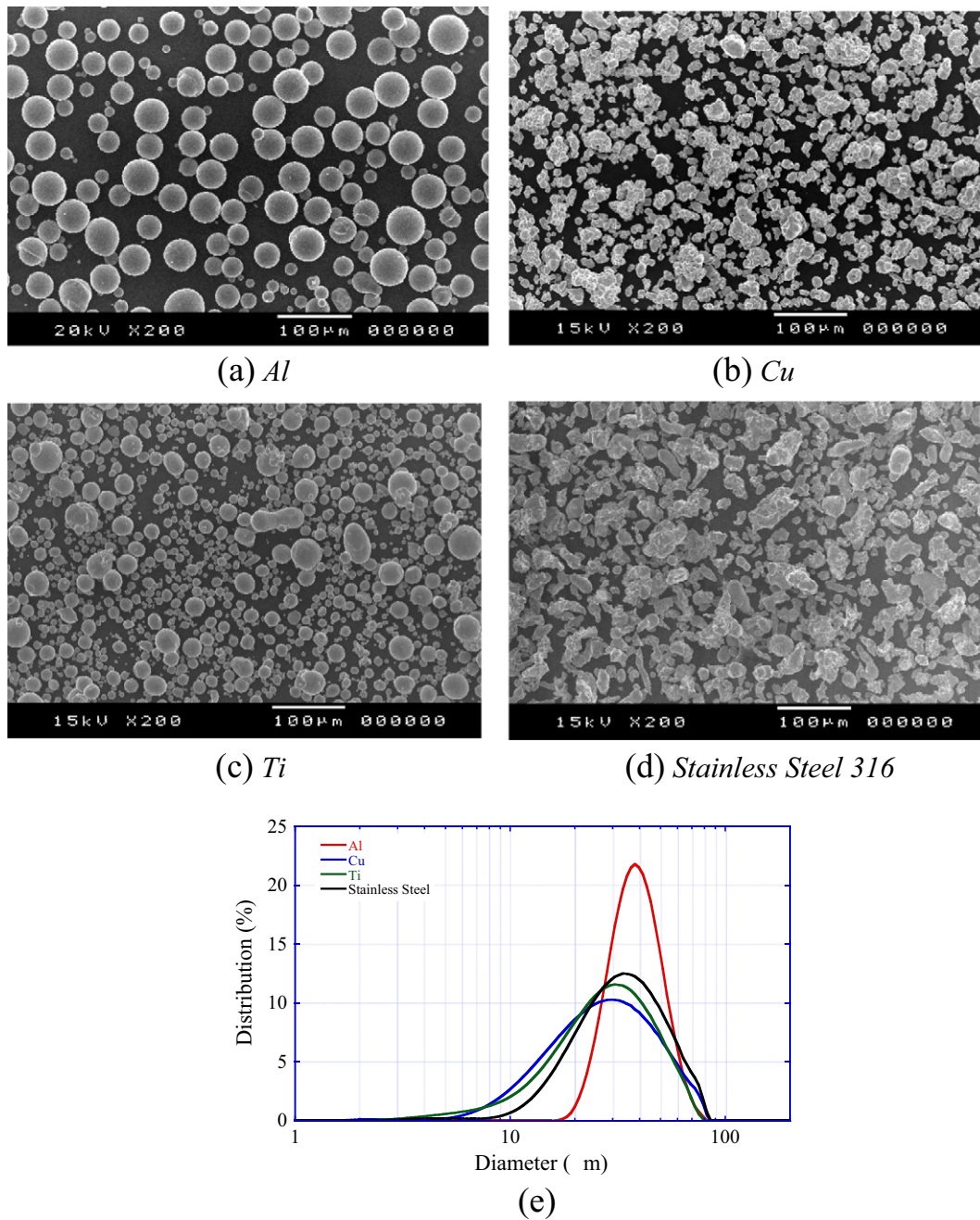


Fig. 1. Morphology of Al (a), Cu (b), Ti (c), stainless steel 316 powder and their diameter distributions (e).

perfect spherical shapes. The pure Cu and stainless steel 316 powders show near spherical shapes. The volume distributions of the particle diameter are shown in Fig. 1(e). Al powder has the narrowest distribution of particle diameter among the four types, with a volume average diameter of about 38 μm . The powder diameter of pure Cu and Ti ranges from 5 to 80 μm , and both of their volume averages are about 30 μm . The powder diameter of stainless steel 316 ranges from 10 to 80 μm , and the volume average of particle diameter is about 35 μm .

A commercial cold spray system, model number PCS-1000 designed by PLASMA GIKEN CO. LTD., was used to prepare the coatings. A convergent–divergent (De-Laval) nozzle was configured to accelerate the working gas to supersonic speed. Nitrogen gas was used as the propellant gas in this test. The spray conditions for cold spray are shown in Table 1. Al alloy cylinder with 100 mm of both outer diameter and length was utilized as the substrate, and more than 5 mm of coatings

were deposited in order to satisfy the dimension of tensile specimen. Fig. 2(a) illustrates the coating preparation process. The cold-sprayed coatings were cut from the substrate, and then machined to a tensile specimen as shown in Fig. 2(b). The detailed dimension of tensile specimen is shown in Fig. 3, and it followed the standard of No. 14B according to JIS Z2201.

Table 1
Spray conditions.

Materials	Al	Cu	Ti	SS316
Gas pressure (MPa)	3			
Gas temperature ($^{\circ}\text{C}$)	380	800	900	800
Powder feed rate (g/min)	25	100	60	100
Spray distance (mm)	30			

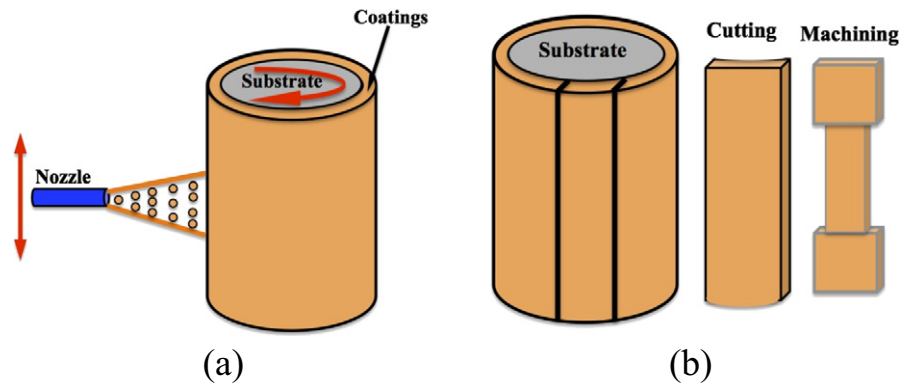


Fig. 2. Preparation of the tensile specimen.

2.2. Heat treatment and tensile test

Heat treatment for the tensile specimen was performed in an argon atmosphere. Table 2 shows the heat treatment conditions. The tensile specimens of as-sprayed and heat-treated coatings were measured with the tensile testing equipment: AG-X (100KN), manufactured by Shimadzu Co., Ltd. Two cameras were equipped with the tensile machine in order to measure the extension of the specimen within the gage length during tensile test.

2.3. Coating characterization

Cross-sections of as-sprayed and heat-treated coatings were prepared vertically to their surfaces by a conventional mechanical polishing method with SiC paper and diamond suspensions. The mirror-polished cross-sections were examined with a digital microscope (VHX-900, Keyence, Japan). The porosity of coatings was measured by image analysis with the cross-section photos. Cu and Ti coatings were etched with 2% nitric acid and 1% fluoric acid respectively before observation. In order to understand the failure mechanism of the cold-sprayed coatings, the fracture surface of the tensile specimens were observed by a field emission scanning electron microscope (JSM-5200LV, JEOL, Japan).

3. Results

3.1. Mechanical properties

Fig. 4 shows the tensile properties of cold-sprayed Al, Cu, Ti and stainless steel 316 coatings. It can be seen that all the as-sprayed coatings have poor ductility and their tensile elongations are less than 0.5%. All the mechanical properties (especially elongation) improved with increase in heat treatment temperature.

For the cold-sprayed Al coatings, the as-sprayed coating has a similar tensile strength as the bulk in spite of the poor elongation. After heat treatment at 200 °C, the cold-sprayed Al coating becomes even stronger,

but still with poor ductility. Further improving the heat treatment temperature to 300 °C, the strength of coating decreases compared to that of heat-treated coating at 200 °C. Nevertheless, it is higher than that of the bulk Al. The coating began to have some ductility with an elongation of about 1.3%. With the increase of heat treatment temperature to more than 400 °C, the coating showed decent ductility and gained more than 10% of elongation. However, the tensile strength of coating decreased and became a little lower than the bulk Al after heat-treating at 400 °C. The most excellent properties of Al coating is the one that was heat-treated at 600 °C. The coating possessed elongation of about 25% (half of the bulk material) and ultimate tensile strength of about 70 MPa (close to the bulk material). However, the yield strength of Al coating after treatment temperature at 600 °C decreased to far lower than the bulk material.

For the cold-sprayed Cu coatings, the as-sprayed coating has a higher tensile strength than the bulk Cu. After heat-treating at 300 °C, the cold-sprayed Cu coating becomes stronger, but with poor ductility (less than 1%). Further raising the heat treatment temperature to 400 °C and 500 °C, excellent mechanical properties were obtained. The tensile strength and elongation of coating even exceed that of bulk Cu. When the heat treatment temperature is increased to 700 °C, the tensile strength and elongation of the coating decreased compared with the ones heat-treated at 400 and 500 °C. It seems that excessive heat treatment can generate adverse effect of improving mechanical properties for cold-sprayed Cu coatings.

For cold-sprayed Ti coatings, the tensile strength and elongation are extremely low compared with that of the bulk Ti (even when heat-treated at a higher temperature of 1000 °C). Generally, the tensile strength of Ti coatings is less than 200 MPa and their elongation is less than 0.5%. It seems that the heat treatment did not significantly improve the mechanical properties of cold-sprayed Ti coatings.

For cold-sprayed stainless steel 316 coatings, the tensile strength and elongation have no improvement compared to that of the as-sprayed coating if the heat treatment temperature is less than 600 °C. When the heat treatment temperature is increased to 800 °C, the tensile strength increased to 300 MPa. However, it still revealed poor ductility (less than 0.5%) because the specimen failed before the plastic deformation stage. With the heat treatment temperature of 1000 °C, the strength of stainless steel 316 coating further increased and some ductility starts to appear. However, strength and elongation are still

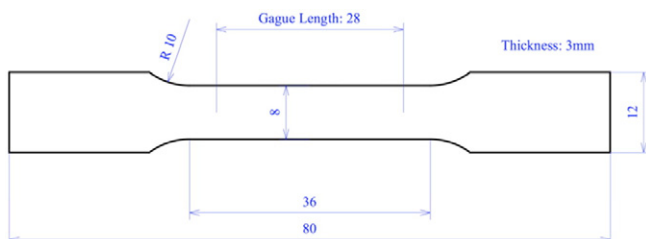


Fig. 3. Dimensions of tensile specimen.

Table 2
Heat treatment conditions.

Materials	Al	Cu	Ti	SS316
Temperature (°C)	200, 300, 400, 600	300, 400, 500, 700	400, 600, 800, 1000	400, 600, 800, 1000
Time (h)	4			

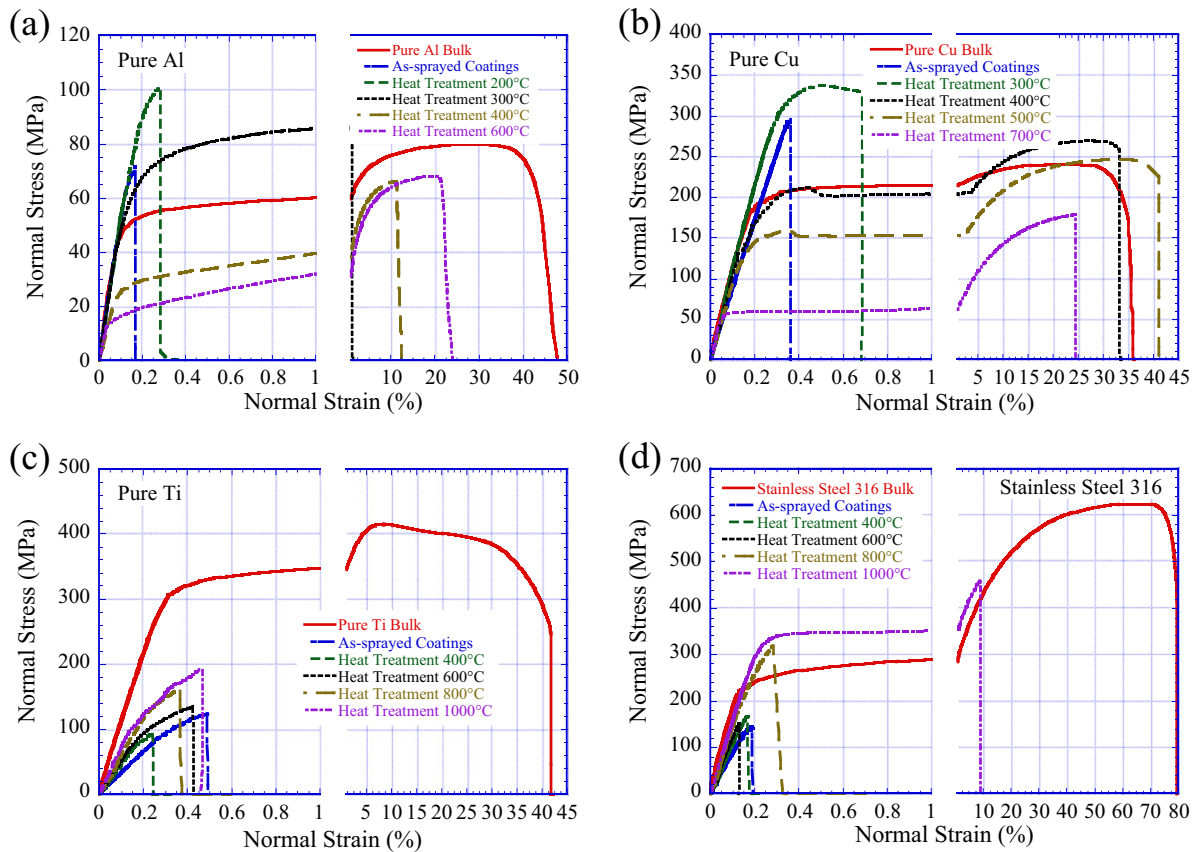


Fig. 4. Tensile properties of cold-sprayed Al (a), Cu (b), Ti (c) and stainless steel 316 (d) coatings.

lower than the bulk since it failed at the early stage of plastic deformation during the tensile test.

3.2. Microstructure

The heat treatment significantly improved the mechanical properties of cold-sprayed Cu. Nevertheless, almost no effects of heat treatment on the mechanical properties of cold-sprayed Ti can be observed (as shown in Fig. 4). To understand the phenomena, microstructures of Cu and Ti were analyzed.

Fig. 5 shows the microstructure of cold-sprayed Cu coatings before and after heat treatment. It can be seen that extremely dense Cu coating was obtained by cold spray. The as-sprayed coating shows that Cu particle deformed intensively during the deposition process owing to the high particle velocity and its excellent ductility. At the same time, grain of Cu particle also deformed during the impact process as shown in Fig. 5(a). After heat treatment of 500 °C, the interface between particles disappeared. The grain of Cu coating after heat treatment at 500 °C looks very uniform and fine. Further improving the heat treatment temperature to 700 °C, the grain of Cu coating becomes coarse compared to that of 500 °C.

Fig. 6 shows the microstructure of cold-sprayed Ti coatings before and after heat treatment. It can be seen that the cold-sprayed Ti coating looks very porous. The as-sprayed coating shows that Ti particle hardly deforms during the deposition process. It seems that Ti particle is too hard to deform during impact. After being heat-treated at 600 °C, some of the interface between particles disappeared, but some still remained. It seems that effective diffusion between the particle interface only happens at closer cohesion of particles. Further improving the heat treatment temperature to 1000 °C, the interface of particles almost disappeared, but some pores inside the coating still remained.

3.3. Fracture surface

After the tensile test, fracture surface was observed by SEM in order to understand its fracture mechanism. Fig. 7 shows the observation location of the fractured specimens.

Fig. 8 shows the fracture surface of Al coatings. For the as-sprayed Al coating, the fracture occurred between the interfaces of particles. No dimple can be observed according to the fractography. It seems that de-cohesive rupture occurred to the as-sprayed Al coating since its cohesion of particles is quite poor without heat treatment. Al coating still fractured at particle interface after heat treatment at 300 °C, even with some diffusion between the particle interfaces as shown in Fig. 8(b). This failure can still be considered as a de-cohesive rupture. Further improving the heat treatment temperature to 600 °C, some dimples can be observed at the fracture surface as shown in Fig. 8(c). It seems that the fracture of the coating belongs to micro-void coalescence rupture because some plastic deformation can be observed. However, some defects can be observed at the fracture surface. This makes the coating fail at its early stage of tensile test and possesses lower tensile strength than that of bulk material. It can be seen that heat treatment cannot fix all of the defects or pores inside the Al coating even with higher heat treatment temperatures.

Fig. 9 shows the fracture surface of Cu coatings. For the as-sprayed Cu coating, the fracture occurred between the interfaces of particles as shown in Fig. 9(a). No dimple can be observed according to the fractography and it seems that particle interface is relatively weak. Consequently, a de-cohesive rupture occurred here for the as-sprayed Cu coating. It can be seen that like Al, brittle failure occurred to the as-sprayed Cu coating, even though it was comparatively dense. After heat-treated at 400 °C, plenty of dimples were observed at the fracture surface. Further improving the heat treatment temperature to 500 °C, dimples at the fracture surface look more uniform. It seems that

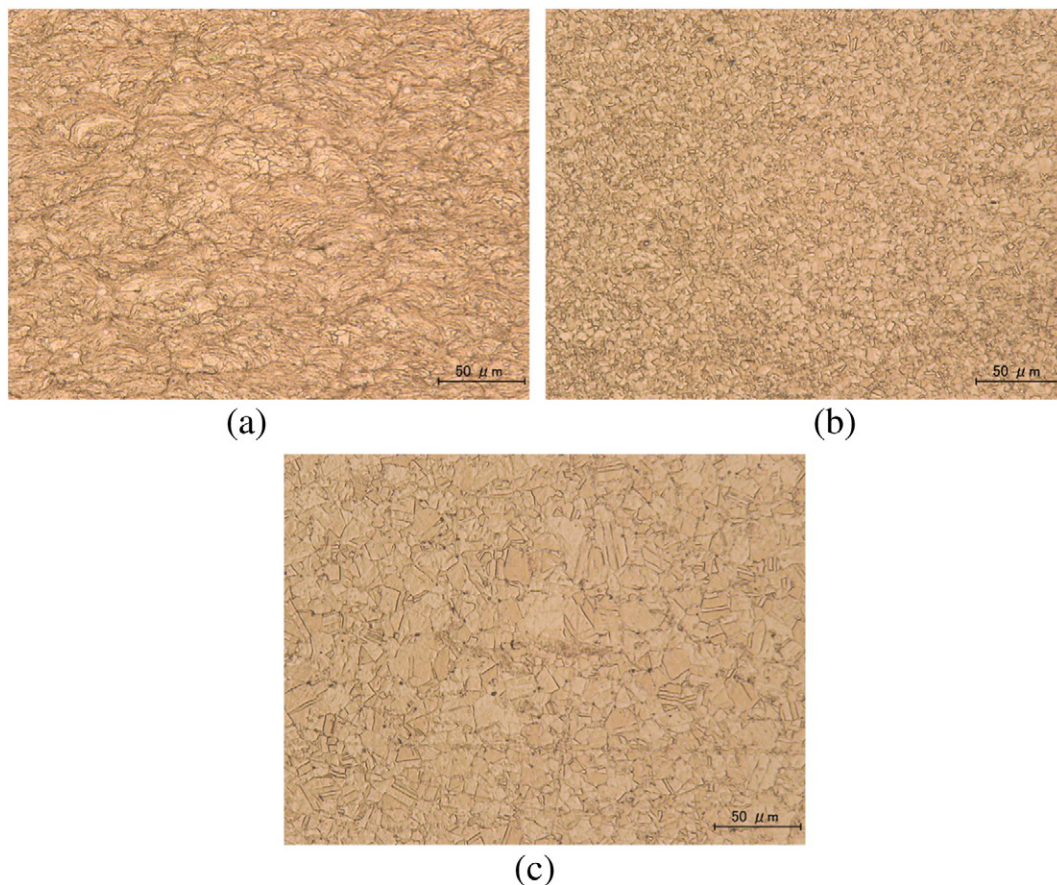


Fig. 5. Microstructure of as-sprayed Cu coatings (a), heat-treated at 500 (b) and 700 °C (c).

fracture in the Cu coatings heat-treated at 400 and 500 °C is due to plastic rupture of micro-void coalescence. When the heat treatment temperature was improved to 700 °C, it can be seen that the size of dimple became larger, and this drops yield and ultimate strength.

Fig. 10 shows the fracture surface of Ti coatings. For the as-sprayed coating, the fracture occurred between the particle interfaces. No dimple can be observed according to the fractography and it can be seen that the brittle de-cohesive rupture occurred to the as-sprayed Ti coating. It seems that the cohesion of particles in the coating is quite poor without heat treatment. The Ti coating still fractured at the particle interface after heat-treated at 600 °C as shown in Fig. 8(b). Compared to the as-sprayed Ti coating, it can be seen that particle interface becomes less visible after heat treatment at 600 °C due to diffusion. However, fracture of the coating can still be considered as a de-cohesive rupture. Further raising the heat treatment temperature to 1000 °C, dimples cannot be observed at the fracture surface. Defects can still be observed at the fracture surface of Ti coating heat-treated at 1000 °C. These defects made the coating fail at an early stage (before entering the plastic deformation stage) during the tensile test. Therefore, the fracture of Ti coating still belongs to brittle de-cohesive rupture after heat treatment at 1000 °C. It seems that heat treatment cannot fix all of defects or pores inside the Ti coating even when the heat treatment temperature is raised to 1000 °C.

Fig. 11 shows the fracture surface of stainless steel 316 coatings. For the as-sprayed stainless steel coating, the fracture occurred between the particle interfaces like the other three materials. The fracture belongs to brittle de-cohesive rupture because no dimple was observed (as shown in Fig. 11(a)). Stainless steel 316 coating still fractured at its particle interface after heat-treating at 600 °C. This time, the fracture surface became rougher than that of the as-sprayed coating. It is possible that fracture went between the weak particle interface and diffusion

happened between some compact particles during heat treatment. The fracture bypassed the diffused particle interface and consequently, made the fracture surface rougher. Further improving the temperature to 1000 °C, some small dimples can be observed at the fracture surface. It seems that fracture of coating belongs to micro-void coalescence rupture because some plastic deformation can be observed. However, some defects can be observed at the fracture surface and this decreases the coating tensile strength. It seems that heat treatment of 1000 °C is still not enough to fix all of the defects inside the stainless steel 316 coating.

4. Discussion

In general, almost no ductility can be observed with the as-sprayed coatings and heat treatment can improve their mechanical properties to a certain extent. In order to discuss the relationship between densification and mechanical properties, porosity of the four as-sprayed coatings were measured. Fig. 12 shows the microstructures of as-sprayed Al and stainless steel coatings. With Figs. 5, 6 and 12, porosity of the as-sprayed coatings can be measured and the results are shown in Table 3. There are two typical coatings: dense (Cu coating) and porous (Ti Coating). These two types of coatings exhibit different mechanical properties compared to their bulk materials. Both the different behaviors of mechanical properties for the four cold-sprayed coatings and their improvements of mechanical properties after heat treatment can be explained by their evolving microstructures.

The evolution of cold-sprayed coatings' microstructure during heat treatment can be summarized as shown in Fig. 13. Two typical cold-sprayed coatings (dense and porous) are shown. If particle velocity is higher and material is ductile, particles deform more and the coating itself becomes dense. In contrast, a porous coating is formed when particle velocity is low and material is hard. The Cu coating can be

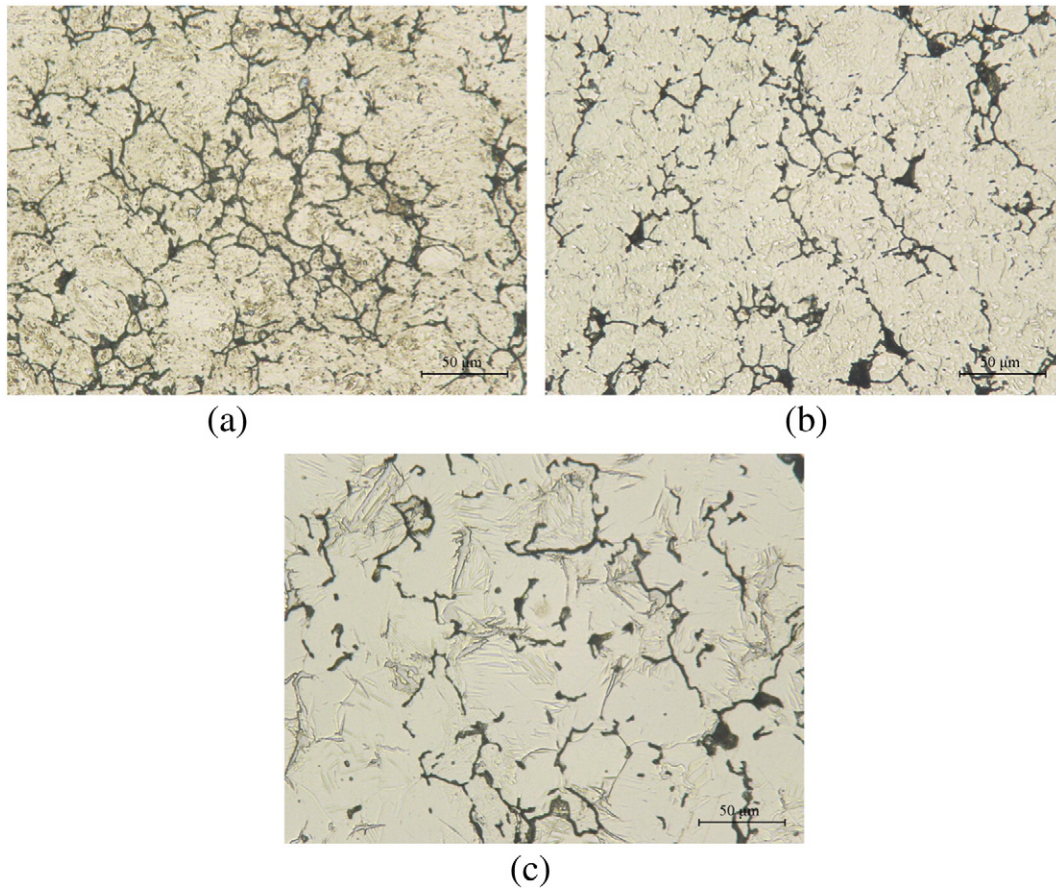


Fig. 6. Microstructure of as-sprayed Ti coatings (a), heat-treated at 600 (b) and 1000 °C (c).

considered as a typical dense coating as shown in Fig. 5. Few defects can be observed in the coating and extremely low porosity of 0.04% was measured. Additionally, intensive work hardening is generated during the impact process of particles. This leads to excellent tensile strength of Cu coating that is even higher than bulk and almost no elongation can be obtained with the as-sprayed Cu coating even though it is extremely dense. The tensile strength of as-sprayed Cu coating is almost determined by the particles interface strength because almost all failure happens here as shown in Fig. 9(a). Cold-sprayed Ti coating can be considered as a relatively porous coating as shown in Fig. 6(a) and porosity of 14.2% was measured. Plenty of defects can be observed in the coating, and this leads to a de-cohesive rupture owing to the failure happened in the early stage of elastic deformation during the tensile test. Its tensile

strength is much less than bulk as shown in Fig. 4(c). For the as-sprayed Al and stainless steel 316 coatings, some defects existed inside as shown in Fig. 12. Consequently, tensile strength of the two materials was decreased by defects. Compared with the bulk materials, the decreased tensile strength of stainless steel coatings is more significant than that of the Al coating as shown in Fig. 4(a) and (d). This is due to porosity in the coatings as shown in Fig. 12 that the stainless steel has more porosity (2.14%) than that in the Al coating (0.87%). The more defects that the coatings may have, the earlier they will fail during the tensile test, consequently a lower tensile strength compared to the bulk materials.

At a lower heat-treating temperature, some diffusion between particles will happen as shown in Fig. 13(b). The interface of particles will become obscure for the dense coating and only the compactly connected interfaces will disappear for the porous coating. This improves the strength of particles interface. However, the work hardening generated during cold spray process still remains in the coatings with lower heat treatment temperature since there are no changes in the grains. Therefore, dense coatings will become stronger but with low ductility. The improved tensile strength of Cu coating heat-treated at 300 °C can attribute to diffusion in the particle interfaces. The same phenomenon can also be observed in Al heat-treated at 200 °C. For stainless steel 316 coating heat-treated at 400 and 600 °C, it is comparatively low and no improvement of tensile strength can be observed (in Fig. 4(d)). Comparing the morphologies of as-sprayed stainless steel coatings with the one heat-treated at 600 °C (in Fig. 11), no significant change can be found. Therefore, sufficient diffusion at particles interface can happen only when the heat treatment temperature is more than 600 °C for stainless steel. The improvement of tensile strength heat-treated at 800 °C proves that there was a significant diffusion at particle interface. In contrast, no significant change of the mechanical properties

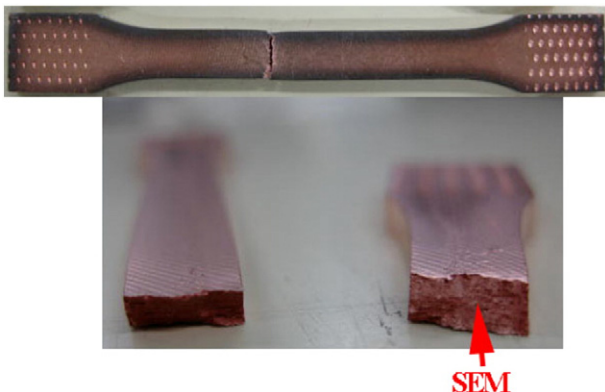


Fig. 7. Observation location of the fractured specimens.

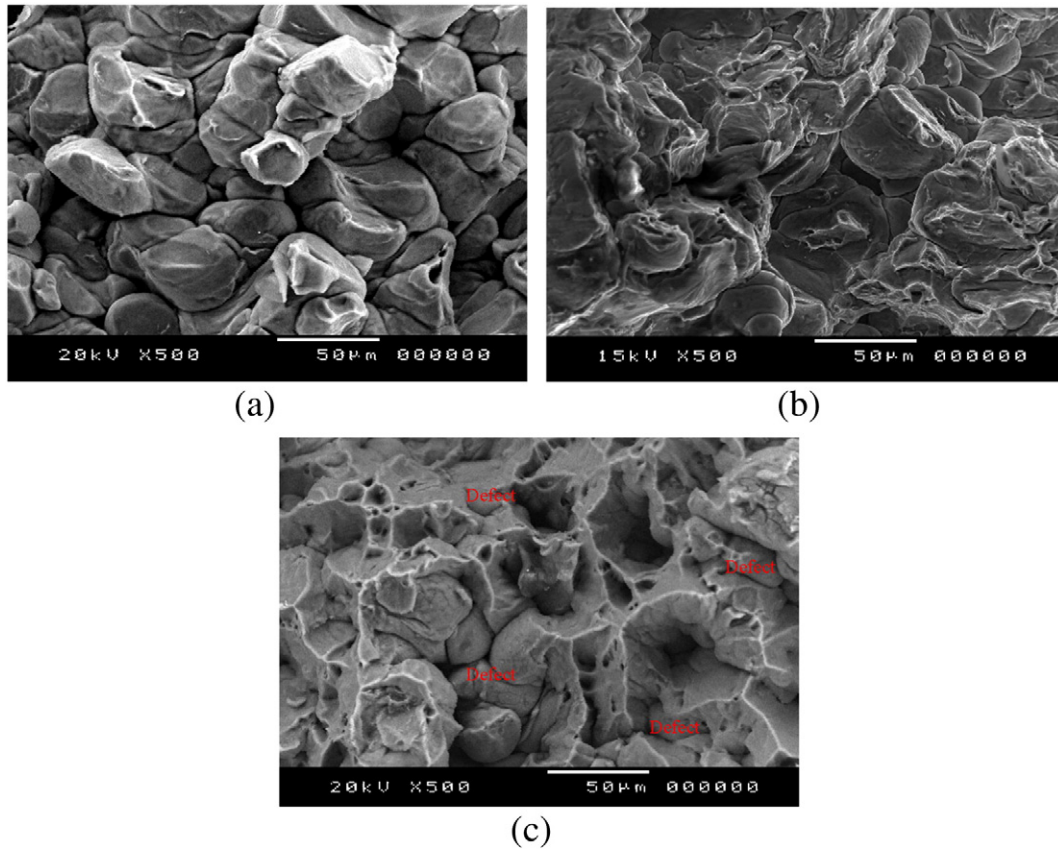


Fig. 8. Fracture surface of as-sprayed Al coatings (a), heat-treated at 300 (b) and 600 °C (c).

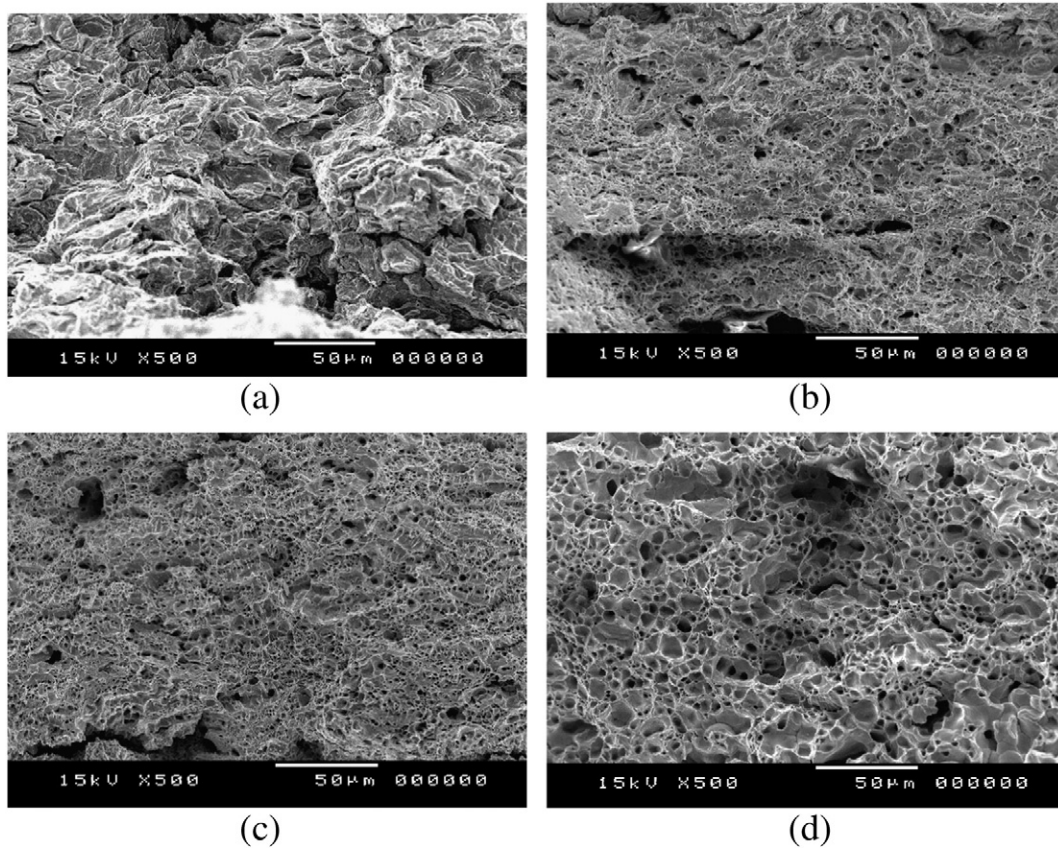


Fig. 9. Fracture surface of as-sprayed Cu coatings (a), heat-treated at 400 (b), 500 (c) and 700 °C (d).

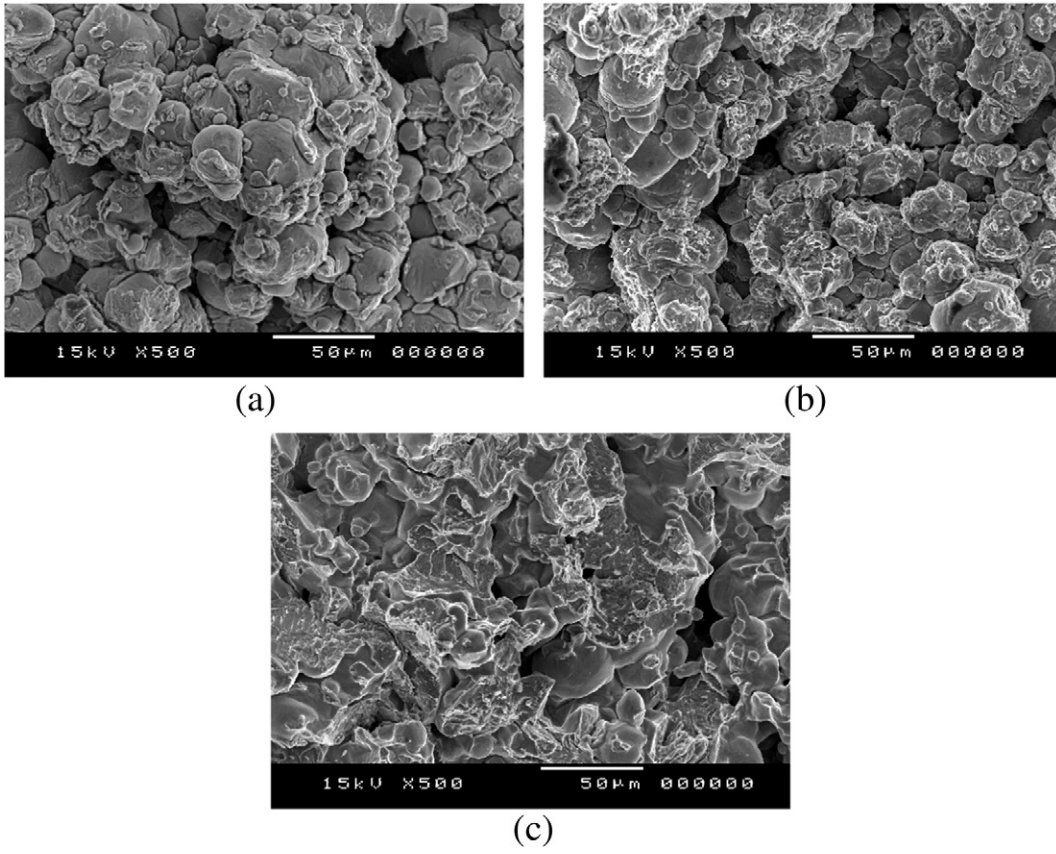


Fig. 10. Fracture surface of as-sprayed Ti coatings (a), heat-treated at 600 (b) and 1000 °C (c).

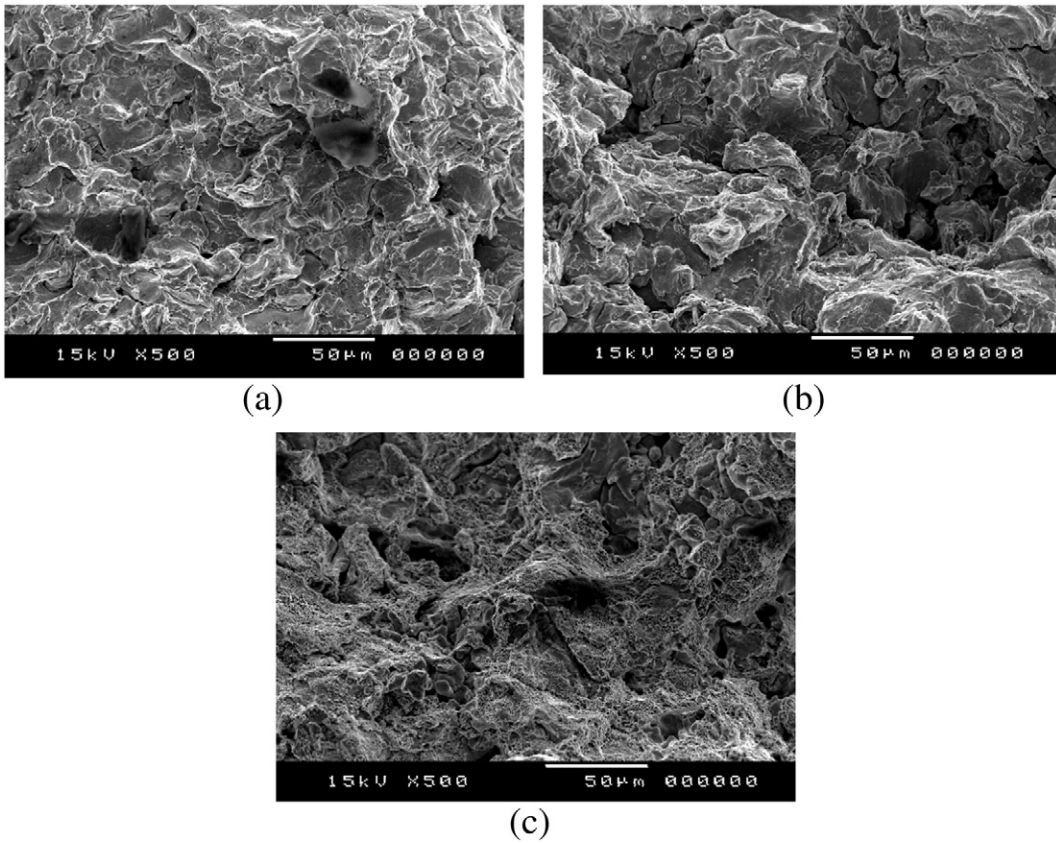


Fig. 11. Fracture surface of as-sprayed stainless steel 316 coatings (a), heat treatment at 600 (b) and 1000 °C (c).

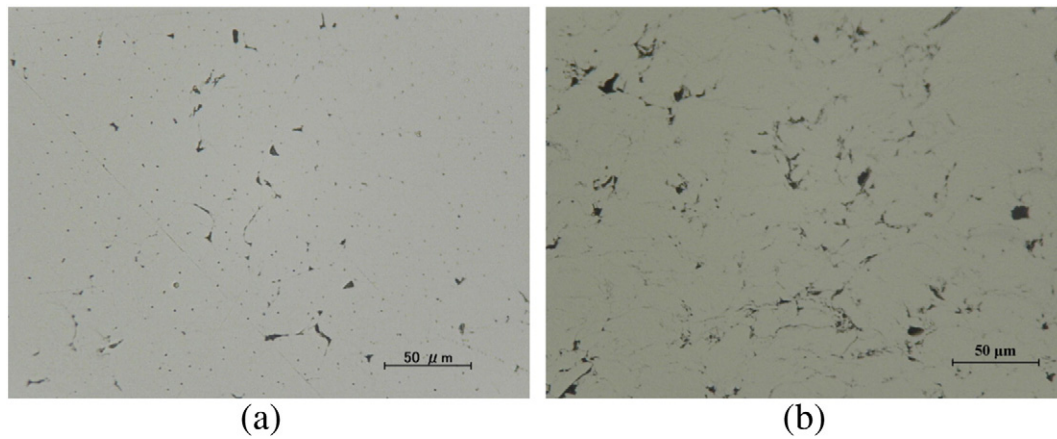


Fig. 12. Microstructure of as-sprayed Al (a) and stainless steel 316 (b) coatings.

will be observed for the porous coatings compared to the as-sprayed coatings because diffusion cannot occur when particles are not bonded strongly. Comparing the microstructures of as-sprayed Ti coating with the one heat-treated at 600 °C in Fig. 6(b), some diffusion were generated at the compact particles interface because some particles interface became less visible. However, the defects in the Ti coating caused the tensile strength to remain still low and there are no significant changes of the tensile strength after heat-treated at 400 and 600 °C.

Further improving the heat treatment temperature, diffusion at the particle interfaces became more intensive and the interfaces completely disappeared. Work hardening and intensive plastic deformation in the coatings generated in the cold spray processing will gradually be removed due to recrystallization during heat treatment (as shown in Fig. 13(c)). Recrystallization for the plastically deformed coating will generate fine grains as shown in Fig. 5(b). From the fractured surface in Fig. 9, it can be seen that recrystallization for Cu coating happened when the heat treatment temperature is over 400 °C; in which corresponded to Kwon's research that recrystallization temperature of Cu is higher than 400 °C [25]. The fine grain of coating leads to good strength and excellent elongation. As shown in Fig. 4(b), it can be better than the bulk in case for Cu. By removing work hardening along with recrystallization, the material restored its ductility and generated a micro-void coalescence rupture during the tensile test. Therefore, plenty of dimples can be observed at the fracture surface as shown in Fig. 9(b) and (c). For stainless steel 316 coating, recrystallization was seen with heat treatment temperature of 1000 °C, since some fine dimples can be observed at the fracture surface (in Fig. 11(c)). Recrystallization temperature of stainless steel 316 in the present studies seems to be a little higher than Hirota's research (from 800 to 950 °C) [26]. It is possible that the porosity in the stainless steel coating has obstructed its diffusion between the particle interfaces during heat treatment and made the recrystallization temperature become a little higher. Although recrystallization brought some elongation to the stainless steel 316 coating heat-treated at 1000 °C, the remained defects led to its rupture at an early stage of plastic deformation during the tensile test since the current heat treatment condition cannot fix all the defects in the coating as shown in Fig. 11(c). Therefore, both tensile strength and elongation of coating are lower than that of the bulk stainless steel. For Al coatings, recrystallization starts at 300 °C. This is where the tensile strength starts

to decrease and some elongation appears as shown in Fig. 4(a). This result is corresponded to Johnson's research that recrystallization temperature of Al is about 300 °C [27]. Unlike Cu, the grain in the Al coating did not become significantly fine because the original grain did not deform much during the deposition process (shown in Fig. 8). Even when the recrystallization happened to the Al coating when heat-treated at 300 °C, the work hardening did not completely remove from the coating. Therefore, coating should have a higher tensile strength and lower elongation compared to the bulk material. Like the stainless steel 316, some defects still remained in the Al coatings as shown in Fig. 8. This will decrease the mechanical properties of Al coating. As a result, Al coating heat-treated at 300 °C has a slightly higher tensile strength and much lower elongation than the bulk material (see Fig. 4(a)). For Ti coating, recrystallization temperature is about 700 °C [28] and heat treatment at 800 and 1000 °C should make the coatings change their mechanical properties. However, since only few particles are deforming, it leads to a small change with the grain during the recrystallization stage as shown in Fig. 6. Diffusion increased the connection strength between the close contact particles, but the

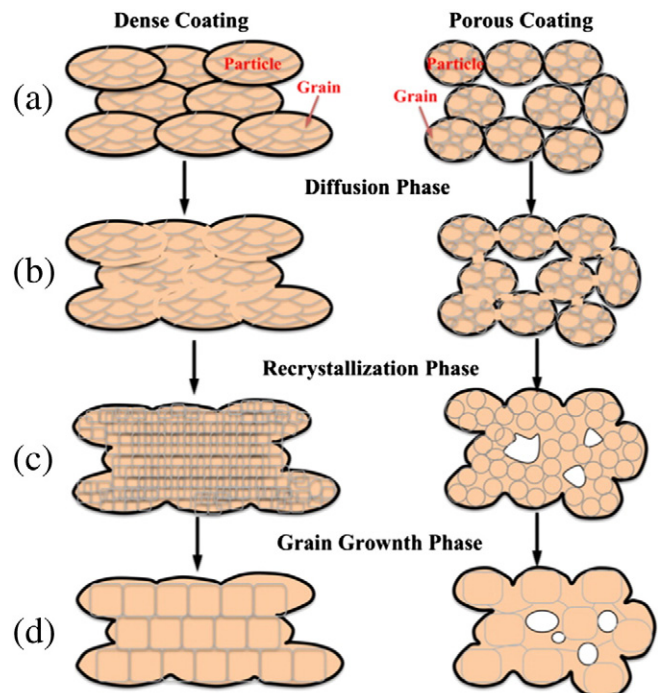


Fig. 13. Schematic of the evolving cold-sprayed coating during heat treatment.

Table 3
Porosity of the as-sprayed coatings.

Materials	Porosity (%)
Al	0.87
Cu	0.04
Ti	14.2
SS 316	2.14

improvement effect becomes quite poor owing to the residual defects (example: big pores). This consequently leads to a brittle de-cohesive rupture as shown in Fig. 10(c). With Ti coating heat-treated at 800 and 1000 °C, poor elongation was obtained and the tensile strength improved a little compared to the as-sprayed coating and far lower than the bulk Ti as shown in Fig. 4(c).

If the heat treatment temperature is too high, the grain will grow as shown in Fig. 13(d). The obvious grain growth happened to the Cu coating heat-treated at 700 °C as shown in Fig. 5. The grown grain can mean that materials can plastically deform easily at lower yield strength. Dimples at the fracture surface became bigger owing to the grain growth as shown in Fig. 9. It can be seen that the grain growth decreased the mechanical properties for dense coatings. For the Al coating, grain growth happened due to the decrease in yield strength with heat treatment of 600 °C. However, Al coating is not as dense as the Cu coating since some porosity existed in the coating. When the heat-treating temperature is higher, it further recovered the defects in the coating and compensated the decrease of mechanical properties caused by the grain growth to some extent. As a result, Al coating heat-treated at 600 °C possesses better elongation than that of 400 °C. For Ti and stainless steel 316 coatings, the heat treatment temperature of 1000 °C is still low to experience the grain growth stage since they have a higher melting point. It can be proved in the Fig. 4(c) and (d) that no decrease in yield strength can be observed for Ti and stainless steel coatings.

Besides mechanical properties of the yield, ultimate strength and elongation, the elastic properties can also be calculated with the stress–strain curve. Table 4 shows the Young's modulus of cold-sprayed coatings derived from Fig. 4. According to Phani and Niyogi's researches, the elastic properties of porous materials are determined by the porosity [29]. The porosity of materials leads to the Young's modulus of porous materials reduced [29,30]. Meanwhile, the cold-sprayed coating always shows lower Young's modulus due to the existence of separated inter-splat boundaries (tiny cracks) [31,32]. For Cu coating, although almost no pores and defects can be observed in the coating (see Fig. 5), its Young's modulus of as-sprayed coating is still about 20% lower than the corresponding bulk material due to the existence of many unbonded inter-splat boundaries as reported in Ref. 31 to 33. After heat treatment at 300 °C, the Young's modulus of coating becomes close to the bulk Cu since the tiny cracks are repaired during heat treatment via diffusion at the inter-splat boundaries. It seems that the tiny cracks in cold-sprayed Cu coatings are almost completely repaired if the heat treatment temperature is higher than 300 °C since the Young's modulus hardly change any more with the higher heat treatment temperatures. For Al coating, the tiny cracks in the coating added its porosity (0.87%) make the Young's modulus of as-sprayed Al coating lower about 25% compared with its bulk material. After heat treatment at 200 and 300 °C, the Young's modulus increases a little owing the disappearance of some tiny cracks. Further improved the heat treatment temperature to 400 and 600 °C, the yield strength decreases significantly and it is difficult to calculate the Young's modulus owing to the short-time elastic stage during the tensile test. For the stainless steel coatings, some pores (2.14%) and separated inter-splat boundaries can be observed (see Fig. 12(b)). Therefore, the as-sprayed coating has a lower

Table 5
Porosity of cold-sprayed Ti coatings.

Heat treatment conditions	Porosity (%)
As-sprayed	14.2
Heat treatment at 600 °C	10.5
Heat treatment at 1000 °C	7.6

Young's modulus than only half of its bulk material as shown in Table 4. The Young's modulus of stainless steel coatings gradually increases with the increase of heat treatment temperature from 400 to 1000 °C. This is caused by the gradual recovery of defects during the heat treatment process, which reduces the density of separated inter-splat boundaries. Heat treatment can also reduce the pores in the cold-sprayed stainless steel 316 coating [23], and this can also increase Young's modulus. However, the Young's modulus of coating after heat treatment at 1000 °C is still a little lower than its bulk material since the bigger cracks (pores) cannot be completely repaired as shown in Fig. 10(c). For Ti coatings, they are so porous that the Young's modulus of as-sprayed coating is far lower than the bulk material as shown in Table 4 (one third), and its Young's modulus gradually rises with the increase of heat treatment temperature like the stainless steel coatings. Table 5 shows the porosity (from Fig. 6) of cold-sprayed Ti coatings. It can be seen that porosity of cold-sprayed Ti coatings decreases after heat treatment because some defects are recovered and some particle boundaries disappeared (see Fig. 6). The Young's modulus in the Ti coating improves when its pores and inter-splat boundaries decreased. However, the Young's modulus of Ti coating heat-treated at 1000 °C is still lower than the corresponding bulk material. Heat treatment can decrease some of the defects inside the Ti coatings, but it cannot eliminate the larger pores (see Fig. 6). Therefore, the Young's modulus cannot reach to the bulk material properties even after heat-treated at 1000 °C.

5. Conclusions

In this study, the mechanical properties of cold-sprayed Al, Cu, Ti and stainless steel 316 coatings were measured and the effects of heat treatment on their mechanical properties were also discussed. It seems that the mechanical properties of cold-sprayed coatings are mainly determined by its microstructure that was formed in cold spray process and changed by the subsequent heat treatment process.

For dense as-sprayed coating such as Cu, the tensile strength is very high, but elongation is poor compared with the bulk material. With lower heat treatment temperature, the cohesive strength of coating improved due to the diffusion between particles, but elongation was less because the work hardening generated during the cold spray process still remained. By increasing the heat treatment temperature, the strength decreased since the work hardening was removed. Also, excellent elongation was possible to obtain because recrystallization was able to restore the grain deformation. It is possible to obtain its best mechanical properties at this stage and it is even better than bulk material. If the heat treatment temperature is too high, it can lead to grain growth. Consequently, lowers the yield or tensile strength.

Table 4
Young's modulus of cold-sprayed coatings and corresponding bulk.

Materials	Young's modulus							
Al	Heat treatment temperature (°C)	As Sprayed	200	300	400	600		Bulk
	Young's modulus (GPa)	52	57.2	54.6	–	–		69.3
Cu	Heat treatment temperature (°C)	As Sprayed	300	400	500	700		Bulk
	Young's modulus (GPa)	84.3	104	103	100	111		107
SS316	Heat treatment temperature (°C)	As Sprayed	400	600	800	1000		Bulk
	Young's modulus (GPa)	85.1	103	117	145	154		183
Ti	Heat treatment temperature (°C)	As Sprayed	400	600	800	1000		Bulk
	Young's modulus (GPa)	32.5	45.8	51.8	57.6	72.8		104

For porous coatings with some defects (like cold-sprayed Al and stainless steel 316 coatings), even if the working hardening generated during cold spray processing improved coating's strength, the tensile strength is still lower than that of bulk materials owing to the defects within the coatings. The phenomenon is more significant with stainless steel 316 coating than that of Al since there were more defects in stainless steel than that in Al coatings. Higher heat treatment temperature effectively fixed the defects in the coatings, which led to obtain better tensile strength. Furthermore improving the heat treatment temperature, the ductility of coatings increased owing to the recrystallization of coating after heat treatment.

For porous coatings with plenty of defects such as Ti, it is difficult to fix all the defects inside the coatings, especially the big pores. The effects of heat treatment on the mechanical properties also look quite poor excluding Young's modulus that is mainly determined by the cohesion of particles. Consequently, the coating's failure always happens at the early elastic deformation stage during the tensile test even when diffusion had been generated. It seems that the tensile strength of Ti coating is mainly determined by these defects. Therefore, the current heat treatment conditions are not sufficient to restore the all the defects and improve the mechanical properties of the porous Ti coating.

References

- [1] A. Papyrin, V. Kosarev, K.V. Klinkov, A. Alkhimov, V.M. Fomin, *Cold Spray Technology*, Elsevier, Oxford, 2006.
- [2] J. Voyer, T. Stoltenhoff, H. Kreye, in: B.R. Marple, C. Moreau (Eds.), *ASM International, Materials Park, OH*, 2003, pp. 71–78.
- [3] E. Calla, D.G. McCartney, P.H. Shipway, in: D. von Hofe (Ed.) *ASM International, Osaka, Japan, May 10–12 2004*, pp. 382–387.
- [4] T. Xiong, Z. Bao, T. Li, Z. Li, in: E. Lugscheider (Ed.), *DVS-Verlag, Düsseldorf, Germany, May 2–4, 2005*, pp. 178–184 (Basel, Switzerland).
- [5] R. Morgan, P. Fox, J. Pattison, C. Sutcliffe, W. O'Neill, *Mater. Lett.* 58 (7–8) (2004) 1317–1320.
- [6] M.K. Decker, R.A. Neiser, D. Gilmore, H.D. Tran, in: C.C. Berndt, K.A. Khor, E.F. Lugscheider (Eds.), *ASM International, Singapore, May 28–30 2001*, pp. 433–439.
- [7] F. Raletz, G. Ezo'o, M. Vardelle, M. Ducos, in: D. von Hofe (Ed.) *ASM International, Osaka, Japan, May 10–12 2004*, pp. 344–349.
- [8] W.-Y. Li, C.-J. Li, G.-J. Yang, *Appl. Surf. Sci.* 257 (5) (2010) 1516–1523.
- [9] D. Morelli, A. Elmoursi, T. Vansteenkiste, D. Gorkiewicz, B. Gillispie, in: B.R. Marple, C. Moreau (Eds.), 1, *ASM International, Orlando, FL*, 2003, pp. 85–90.
- [10] H.-T. Wang, C.-J. Li, G.-J. Yang, C.-X. Li, *Vacuum* 83 (2009) 146–152.
- [11] J. Karthikeyan, C.M. Kay, J. Lindemann, in: C.C. Berndt, K.A. Khor, E.F. Lugscheider (Eds.), *ASM International, Singapore, May 28–30 2001*, pp. 383–387.
- [12] R.S. Lima, J. Karthikeyan, C.M. Kay, J. Lindemann, C.C. Berndt, *Thin Solid Films* 416 (2002) 129–135.
- [13] G.-J. Yang, C.-J. Li, F. Han, W.-Y. Li, A. Ohmori, *Appl. Surf. Sci.* 54 (13) (2008) 3979–3982.
- [14] W.-Y. Li, C.-J. Li, H. Liao, *J. Therm. Spray Technol.* 15 (2) (2006) 206–211.
- [15] F. Gärtner, T. Stoltenhoff, J. Voyer, H. Kreye, S. Riekehr, M. Koçak, *Surf. Coat. Technol.* 200 (24) (2006) 6770–6782.
- [16] Z. Arabgol, H. Assadi, T. Schmidt, F. Gärtner, T. Klassen, *J. Therm. Spray Technol.* 23 (1–2) (2014) 84–90.
- [17] R. Ghelichi, S. Bagherifard, D. MacDonald, I. Fernandez-Pariente, B. Jodoin, M. Guagliano, *Appl. Surf. Sci.* 288 (1) (2014) 26–33.
- [18] K. Spencer, V. Luzin, N. Matthews, M.-X. Zhang, *Surf. Coat. Technol.* 206 (19–20) (2012) 4249–4255.
- [19] V. Luzin, K. Spencer, M.-X. Zhang, *Acta Mater.* 59 (3) (2011) 1259–1270.
- [20] P. Sudharshan Phani, D. Srinivasa Rao, S.V. Joshi, G. Sundararajan, *J. Therm. Spray Technol.* 16 (3) (2007) 425–434.
- [21] S. Feng, C. Wang, B. Ma, G. Ling, Z. Zheng, *2nd International Conference on Electronic & Mechanical Engineering and Information Technology*, Atlantis Press, Paris, France, 2012, pp. 1460–1464.
- [22] X.-M. Meng, J.-B. Zhang, W. Han, J. Zhao, Y.-L. Liang, *Appl. Surf. Sci.* 258 (2) (2011) 700–704.
- [23] B. AL-Mangour, P. Vo, R. Mongrain, E. Irissou, S. Yue, *J. Therm. Spray Technol.* 23 (4) (2014) 641–652.
- [24] W. Wong, E. Irissou, P. Vo, M. Sone, F. Bernier, J.-G. Legoux, H. Fukunuma, S. Yue, *J. Therm. Spray Technol.* 22 (2–3) (2013) 413–421.
- [25] D. Kwon, H. Park, S. Ghosh, C. Lee, *J. Korean Phys. Soc.* 44 (5) (2004) 1108–1112.
- [26] N. Hirota, F. Yin, T. Inoue, T. Azuma, *ISIJ Int.* 48 (4) (2008) 475–482.
- [27] G. Johnson, *Recovery and recrystallization behaviour of AA5754 and IF-Boron steel during annealing*, Master thesis of the University of British Columbia, 2001, 71.
- [28] K. Hajizadeh, S. Ghobadi Alamdari, B. Eghbali, *Physica B* 417 (2013) 33–38.
- [29] K.K. Phani, S.K. Niyogi, *J. Mater. Sci. Lett.* 6 (5) (May 1987) 511–515.
- [30] J. Kovacic, *J. Mater. Sci. Lett.* 18 (1999) 1007–1010.
- [31] G. Sundararajan, P. Sudharshan Phani, A. Jyothirmayi, Ravi C. Gundakaram, *J. Mater. Sci.* 44 (9) (May 2009) 2320–2326.
- [32] G. Sundararajan, Naveen M. Chavan, S. Kumar, *J. Therm. Spray Technol.* 22 (8) (December 2013) 1348–1357.